

# Rest-to-Rest Motion of a One-link Flexible Arm with Smooth Bang-Bang Torque Profile

Alessandro De Luca and Heiko Panzer

**Abstract** We consider the problem of finding a torque input command that achieves rest-to-rest motion in given time for a one-link flexible arm, avoiding residual vibrations. In [7], we presented a method based on the definition of a system output having maximum relative degree (flat output), the planning of an interpolating polynomial trajectory for this output, and inverse dynamics computation of the required torque. However, the more flexible modes are considered, the higher becomes the order of the polynomials required in the trajectory planning step. This results in a peaking velocity effect, with very slow start and arrival phases, and thus in a waste of time and/or of useful torque capacities. A novel solution will be presented that enables to approximately minimize the transfer time under a maximum torque constraint or minimize the torque needed for a given motion time. We modify the previous method so as to generate torque profiles of the bang-bang type, but with smooth interpolating phases near the start, midpoint, and final instants. The method is illustrated for an Euler-Bernoulli beam model of a one-link flexible arm with dynamic boundary conditions. Numerical results show the large benefits obtained with this solution.

## 1 Introduction

One of the current trends in the design of robotic arms concerns the use of lightweight materials [3]. This allows to reduce the torque needed to perform a given motion task, and thus the size and cost of the robot actuators, or to increase the operational speed with the given motor capabilities. Lightweight robots, however, typically display flexibility distributed along long/slender links. When such flexibility is not accounted for in the design of motion controllers, several drawbacks are encountered.

---

Alessandro De Luca, Heiko Panzer  
Dipartimento di Informatica e Sistemistica, Università di Roma "La Sapienza", Via Ariosto 25,  
00185 Roma, Italy. e-mail: deluca@dis.uniroma1.it, heiko.panzer@gmx.de

Steady-state errors typically result when performing end-effector regulation tasks, because of the static deflection of the arm due to gravity. Moreover, dynamic oscillations occur along nominal (in particular, fast) trajectories, induced by the rigid body-flexible dynamics interaction, and instability phenomena arise in tasks involving contact with the environment [4, 5]. Feedback control design, especially when based on a reliable dynamic model of the flexible arm, may compensate for most of such errors at the expense of additional sensorization (strain gauges, accelerometers, etc.) needed for measuring the current deflection state of the structure [11]. Still, the design of nominal commands to be used as feedforward terms in the control law is an open area of research. In principle, one would like to compute an open-loop torque that enables exact completion of a desired motion task, while accounting for link flexibility [6].

In particular, when addressing the problem of rest-to-rest motion for flexible arms, i.e., executing a slew maneuver between two given configurations of equilibrium in prescribed time, at the nominal final time one has to cope with residual vibrations, which have been excited during the gross motion [1]. While these may eventually vanish thanks to the structural damping of the modes or to the damping injected by feedback, the practical result is a degradation of performance in terms of traveling time and final accuracy. This becomes particularly critical when time-optimal reconfigurations are sought, under maximum torque (and possibly, velocity) constraints. For one-link flexible arms characterized by linear dynamics, two popular model-based techniques that have addressed the rest-to-rest motion problem are based on input shaping [15] and on inverse dynamics trajectory design [12]. The first approach filters out from a step input reference command the main characteristic frequencies of the system, but is not able to handle a large number of flexible modes. The second approach leads to non-causal solutions, with a resulting motion completion time that cannot be determined accurately a priori.

In [7], we introduced a new rest-to-rest motion planning method based on the definition of a suitable system output  $y$  having maximum relative degree (or, equivalently, associated to a transfer function with no zeros). This output, which is referred to also as *flat* [10], always exists for controllable linear systems and can be computed in closed form once a standard dynamic model of a flexible arm is available, as opposed to the previous numerical approach presented in [16] which suffered from ill-conditioning in the presence of a large number of relevant modes. As a matter of fact, the dynamical state of the flexible arm can be equivalently represented in terms of  $y$  and its derivatives. Designing a polynomial trajectory for this specific output that interpolates suitable boundary conditions including high-order derivatives, the motion task can be realized in the prescribed time and the associated input torque command can be obtained by an explicit inverse dynamics computation. In [9], this approach has been extended with the inclusion of viscous friction and modal damping, and experimentally verified on a one-link flexible arm made of a thin harmonic steel beam. Interestingly, since the original method is defined in the time domain, it has been possible to apply it also to some multi-link flexible robots with nonlinear dynamics (see [8, 10]).

The main drawback of the method resides in the choice of polynomial interpolation for planning the trajectory of the output variable  $y$ . This simple class of functions is well suited for interpolating symmetric, zero conditions at the initial ( $t = 0$ ) and final ( $t = T$ ) time on the first and further time derivatives of  $y$ , without generating overshoot or wandering between the start and goal configurations. The zero values imposed to the time derivatives of  $y$  at the motion boundaries are strictly associated to the rest-to-rest nature of the desired motion task, while the highest order of involved derivatives of  $y$  depends on the number of considered flexible modes. However, the obtained profile  $y_d(t)$  as well as the related nominal torque  $\tau_d(t)$ , will typically have very ‘soft’ start and arrival phases, resulting in a peaking velocity effect at the motion midpoint and in a waste of useful torque capacity. This becomes particularly evident when considering the presence of a large number of flexible modes, i.e., when very high-order interpolating polynomials need to be used. In the presence of a maximum torque bound, this will require a longer transfer time with the torque being saturated only in one single instant (at the midpoint).

In this paper, a novel solution will be presented that enables to approximately minimize the transfer time under a given torque constraint or, in a rather equivalent way, to minimize the maximum torque needed for a given motion time. The original approach is modified so as to generate torque profiles of the bang-bang type, but with smooth interpolating phases near the start, midpoint, and final instants. When planning the parts of the trajectory that belong to these phases, we shall still take advantage of the convenient properties of the flat output  $y$ . As a result, residual vibrations will be likewise prevented at the final time while actuator capacity will be used in an almost optimal way.

It should be mentioned that the generation of smooth torque profiles of this kind is a common practice in industry for rigid robot arms and other motion control problems. The novelty here is two-fold: *i*) an explicit use in the trajectory design of the flexible model of the arm, which allows to account for the full vibration properties of the structure; *ii*) the trajectory planning is made on a suitable output (corresponding to the angular position of a particular point along the flexible arm) in place of the common choices of the clamped joint (actuator) or tip (load) variables, leading to straightforward computations. We note also that our design applies to an arbitrary large number of flexible modes (for comparison, see, e.g., [13] on the use of interpolating polynomials for cam design including only the first few modes of vibration).

The method is illustrated for an Euler-Bernoulli beam model of a one-link flexible arm, with dynamic boundary conditions [2], described in Sect. 2. Section 3 recalls the definition and computation of a flat output  $y$  and the associated inverse dynamics computation of the input torque  $\tau$ . The design of a smooth bang-bang torque profile is addressed in Sect. 4, while in Sect. 5 we report some representative numerical results. In the concluding Sect. 6, we highlight also possible future developments.

## 2 Dynamic modeling

Consider an arm with a single rotating flexible link of length  $\ell$  and uniform linear mass density  $\rho$  moving on the horizontal plane. We assume small bending deformations limited to the plane of motion. The arm is driven by an electrical actuator at the base, having inertia  $J_0$  and producing a torque  $\tau$ , and carries a tip payload of mass  $M_p$  and inertia  $J_p$ . Let the variable  $\theta$  be the angle between the rotating coordinate axis  $x$ , pointing to the instantaneous center of mass of the link, and the inertial frame (see Fig. 1). We model the flexible link as an Euler-Bernoulli beam with Young modulus  $E$  and inertia of the cross section  $I$ . The transversal bending deformation at a point  $x \in [0, \ell]$  is described by  $w(x, t)$ .

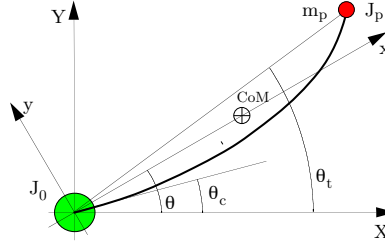


**Fig. 1** A one-link planar flexible arm with definition of variables

From the Euler-Bernoulli assumption, using balance of shear forces and moments, we obtain two mixed ordinary/partial differential equations governing the flexible arm dynamics, with geometric and dynamic boundary conditions involving the system parameters [2]. These can be solved by separation in space and time, expressing  $w(x, t)$  in terms of a finite number  $n_e$  of deformation mode shapes  $\phi_i(x)$  with associated deformation coordinates  $\delta_i(t)$ ,

$$w(x, t) = \sum_{i=1}^{n_e} \phi_i(x) \delta_i(t). \quad (1)$$

Accordingly, denoting by a prime ( $'$ ) the spatial derivative w.r.t.  $x$ , the free evolution ( $\tau(t) \equiv 0$ ) of the system is characterized by the following ordinary differential equations

$$EI \phi_i''''(x) - \rho \omega_i^2 \phi_i(x) = 0, \quad (2)$$

$$\ddot{\delta}_i(t) + \omega_i^2 \delta_i(t) = 0, \quad (3)$$

$\omega_i$  being the  $i$ -th eigenfrequency of the flexible arm, for  $i = 1, \dots, n_e$ . The spatial boundary conditions for (2) are

$$\begin{aligned}\phi_i(0) &= 0 & EI\phi_i''(0) + \omega_i^2 J_0 \phi_i'(0) &= 0 \\ EI\phi_i''(\ell) - \omega_i^2 J_p \phi_i'(\ell) &= 0 & EI\phi_i'''(\ell) + \omega_i^2 M_p \phi_i(\ell) &= 0,\end{aligned}$$

whereas for (3), suitable initial time conditions  $\delta_i(0) = \delta_{i0}$ ,  $\dot{\delta}_i(0) = \dot{\delta}_{i0}$  can be chosen ( $\delta_{i0} = \dot{\delta}_{i0} = 0$ , for  $i = 1, \dots, n_e$ , when the arm is initially at rest).

To fulfill (2), the general solutions are in the form (mode shapes)

$$\phi_i(x) = A_i \sin(\beta_i x) + B_i \cos(\beta_i x) + C_i \sinh(\beta_i x) + D_i \cosh(\beta_i x), \quad (4)$$

where  $\beta_i = \sqrt[4]{\rho \omega_i^2 / EI}$  are the first  $n_e$  roots of the *characteristic equation*

$$\begin{aligned}(csh - sch) - \frac{2M_p}{\rho} \beta_i s sh - \frac{2J_p}{\rho} \beta_i^3 c ch - \frac{J_0}{\rho} \beta_i^3 (1 + c ch) \\ - \frac{M_p}{\rho^2} \beta_i^4 (J_0 + J_p)(csh - sch) + \frac{J_0 J_p}{\rho^2} \beta_i^6 (csh + sch) - \frac{J_0 J_p M_p}{\rho^3} \beta_i^7 (1 - c ch) = 0,\end{aligned}$$

with  $s = \sin(\beta_i \ell)$ ,  $c = \cos(\beta_i \ell)$ ,  $sh = \sinh(\beta_i \ell)$ , and  $ch = \cosh(\beta_i \ell)$ . Every mode shape is defined up to a constant factor, each of which is obtained by suitable orthonormality conditions.

Using an energy approach, the Euler-Lagrange equations are written in terms of the  $n_e + 1$  generalized coordinates  $\mathbf{q} = [\theta, \delta_1, \dots, \delta_{n_e}]^T$  and provide the linear (and controllable) dynamic model of the flexible arm as

$$J \ddot{\theta} = \tau, \quad (5)$$

$$\ddot{\delta}_i + \omega_i^2 \delta_i = \phi_i'(0) \tau, \quad i = 1, \dots, n_e, \quad (6)$$

where  $J = J_0 + J_p + M_p \ell^2 + (\rho \ell^3)/3$  is the total inertia of the arm w.r.t. the joint axis. Dissipative effects can be included in the model (5–6), see, e.g., [9], but are not considered here for simplicity.

### 3 Definition of a flat output

For system (5–6), it has been shown in [7] that one can always define an output function of the form

$$y(t) = \theta(t) + \sum_{i=1}^{n_e} c_i \delta_i(t) \quad (7)$$

and choose the coefficients  $c_i$  so that  $y(t)$  and its first  $2n_e + 1$  time derivatives are independent of  $\tau(t)$ , which appears in turn only in the  $2(n_e + 1)$ -th time derivative (this output has then maximum relative degree). This occurs if and only if the coefficients in (7) are chosen as

$$c_i = -\frac{1}{J\phi_i'(0)} \prod_{\substack{j=1 \\ j \neq i}}^{n_e} \frac{\omega_j^2}{\omega_j^2 - \omega_i^2}, \quad i = 1, \dots, n_e, \quad (8)$$

which is always well defined since  $\omega_i \neq \omega_j$  for  $i \neq j$ . Accordingly, the transfer function from the input  $\tau$  to the flat output  $y$  should have no zeros and is found indeed to be (by using Laplace transforms)

$$\frac{y(s)}{\tau(s)} = \frac{\prod_{i=1}^{n_e} \omega_i^2 / J}{s^2 \prod_{i=1}^{n_e} (s^2 + \omega_i^2)}. \quad (9)$$

Thanks to its properties, we can use the flat output  $y$  together with its derivatives up to order  $2n_e + 1$  as a new state representation of the system, linked to the generalized coordinates  $\mathbf{q}$  and their derivatives  $\dot{\mathbf{q}}$  by

$$\begin{bmatrix} y \\ \dot{y} \\ \vdots \\ y^{[2n_e]} \end{bmatrix} = Q \begin{bmatrix} \theta \\ \delta_1 \\ \vdots \\ \delta_{n_e} \end{bmatrix}, \quad \begin{bmatrix} \dot{y} \\ y^{[3]} \\ \vdots \\ y^{[2n_e+1]} \end{bmatrix} = Q \begin{bmatrix} \dot{\theta} \\ \dot{\delta}_1 \\ \vdots \\ \dot{\delta}_{n_e} \end{bmatrix}, \quad (10)$$

with the invertible matrix

$$Q = \begin{bmatrix} 1 & c_1 & \dots & c_{n_e} \\ 0 & -c_1 \omega_1^2 & \dots & -c_{n_e} \omega_{n_e}^2 \\ \dots & \dots & \dots & \dots \\ 0 & (-1)^{n_e} c_1 \omega_1^{2n_e} & \dots & (-1)^{n_e} c_{n_e} \omega_{n_e}^{2n_e} \end{bmatrix}.$$

In particular, this mapping defines the appropriate boundary conditions for  $y$  and its derivatives associated to any desired value of the state  $(\mathbf{q}, \dot{\mathbf{q}})$  at the initial and final time.

For a generic state-to-state transfer in time  $T$ , one can first generate a sufficiently smooth interpolating trajectory  $y = y_d(t)$  using these boundary conditions at time  $t = 0$  and  $t = T$ , and then compute the nominal torque  $\tau = \tau_d(t)$  that executes the desired motion by inverse dynamics. This is obtained by imposing  $y^{[2(n_e+1)]} = y_d^{[2(n_e+1)]}$  in the expression of the highest order derivative of the flat output  $y$  and solving for  $\tau$ :

$$\tau_d(t) = \frac{y_d^{[2(n_e+1)]}(t) - (-1)^{n_e+1} \sum_{i=1}^{n_e} c_i \omega_i^{2(n_e+1)} \delta_i(t)}{(-1)^{n_e} \sum_{i=1}^{n_e} c_i \omega_i^{2n_e} \phi_i'(0)}, \quad (11)$$

with  $t \in [0, T]$ . In eq. (11), the values of  $\delta_i$ ,  $i = 1, \dots, n_e$  are obtained either algebraically, by inverting the linear system of equations (10) with  $y \equiv y_d(t)$ , or by

simple numerical integration, simulating the flexible arm dynamics (5–6) under the input command (11).

#### 4 Smooth bang-bang torque profile

In a rest-to-rest motion for a one-link flexible arm modeled by eqs. (5–6), the arm should be moved from an initial undeformed configuration  $\mathbf{q}_i = [\theta_i, \mathbf{0}^T]^T$  at  $t = 0$  to a final undeformed configuration  $\mathbf{q}_f = [\theta_f, \mathbf{0}^T]^T$  at a prescribed time  $T$ , with  $\dot{\mathbf{q}}(0) = \dot{\mathbf{q}}(T) = \mathbf{0}$ . Indeed, the motion task is independent of the particular value of  $\theta_i$  (which can be thus set to 0, without loss of generality) but only on  $\Delta\theta = \theta_f - \theta_i$ . The final time  $T$  can also be seen as a free parameter to be minimized under the maximum torque constraint  $|\tau(t)| \leq \tau_{\max}$ , for  $t \in [0, T]$ .

For the rest-to-rest motion case, using the structure of eqs. (10), the appropriate boundary conditions for an interpolating trajectory  $y = y_d(t)$  are simply:  $y_d(0) = \theta_i$ ,  $y_d(T) = \theta_f$ , with all derivatives up to the  $(2n_e + 1)$ -th equal zero at the initial and final time. For satisfying these boundary conditions, a (symmetric) polynomial of degree  $4n_e + 3$  will be sufficient. Moreover, setting to zero also the  $(2n_e + 2)$ -nd derivative of  $y_d$  and using a polynomial of degree  $4n_e + 5$  will guarantee that the required torque starts and ends at zero. Similarly, higher order polynomials lead to incremental smoothness of the torque profile.

In any event, a more direct expression of the rest-to-rest motion torque can be obtained now in closed form without the need of computing neither the coefficients  $c_i$  nor  $Q$  or its inverse (as needed instead in eq. (11)). In fact, inverting eq. (9) for  $y = y_d$  yields

$$\tau(s) = \frac{J}{\prod_{i=1}^{n_e} \omega_i^2} \left[ s^2 \prod_{i=1}^{n_e} (s^2 + \omega_i^2) \right] y_d(s).$$

In the time domain, this results in

$$\tau(t) = \frac{J}{\prod_{i=1}^{n_e} \omega_i^2} \left[ y_d^{[2n_e+2]}(t) + \sum_{i=0}^{n_e-1} \alpha_i y_d^{[2i+2]}(t) \right]. \quad (12)$$

The  $n_e$  coefficients  $\alpha_i$  are obtained by convolution of the polynomials  $(s^2 + \omega_i^2)$ . For example, for  $n_e = 3$ , we have

$$\alpha_0 = \omega_1^2 \omega_2^2 \omega_3^2, \quad \alpha_1 = \omega_1^2 \omega_2^2 + \omega_1^2 \omega_3^2 + \omega_2^2 \omega_3^2, \quad \alpha_2 = \omega_1^2 + \omega_2^2 + \omega_3^2.$$

It turns out, however, that to perform a certain movement in a given motion time, the peak value required with the torque profile based on polynomial interpolation for the flexible link fairly exceeds the piece-wise constant value of the bang-bang torque needed for a mass-equivalent rigid link, i.e., modeled just by eq. (5). This happens due to the extremely slow initial and final phases that can be seen in Fig. 2(a),

with an associated waste of actuator capacity. Including more flexible modes worsen the picture, since it means using higher order polynomials for the flat output, and accordingly more zero boundary conditions on its higher derivatives.

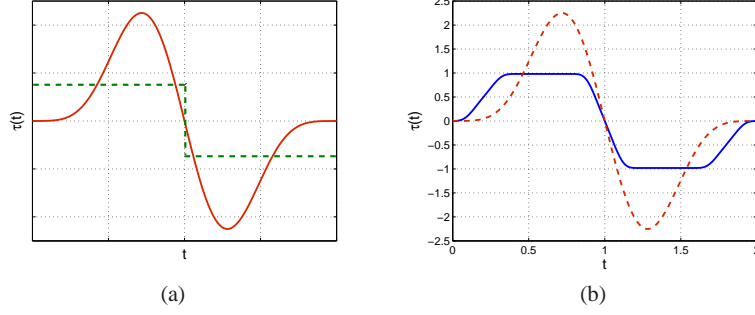


**Fig. 2** (a) Polynomial torque for a flexible link vs. bang-bang torque (- -) for a mass-equivalent rigid link; (b) Polynomial torque vs. smoothed bang-bang torque (-) for the same flexible link

When considering a maximum torque bound  $\tau_{\max}$ , we would like to take advantage of the bang-bang torque profile that yields minimum transfer time for the equivalent rigid link, but still avoid that the presence of flexibility generates residual vibrations that prolong motion completion time. In the rigid case, we have indeed the relationship

$$\Delta\theta = \theta_f - \theta_i = \frac{1}{4J} \tau_{\max} T_{\min}^2, \quad (13)$$

between the total displacement  $\Delta\theta$ , the maximum torque  $\tau_{\max}$ , and the minimum motion time  $T_{\min}$ . The basic idea is then to smoothen the initial, midpoint, and final transitions to the maximum absolute value of the torque, by exploiting respectively the rest-to-state, state-to-state, and state-to-rest features of the polynomial interpolation based on the flat output (7). The possible outcome is shown in the right side of Fig. 2, where the motion time  $T$  and the total displacement  $\Delta\theta = \Delta y$  have been fixed and a much lower torque profile is obtained in comparison to the polynomial interpolation case.

During the phases at constant maximum (positive or negative) torque, the link deformation is constant and we know from eq. (6)

$$|\delta_i(t)| = \frac{\phi_i'(0) \tau_{\max}}{\omega_i^2} =: \bar{\delta}_i (= \text{const}), \quad i = 1, \dots, n_e. \quad (14)$$

From eq. (10), it follows that all derivatives of  $y$  with odd degree between 3 and  $2n_e + 1$  should be zero, since in these phases  $\dot{\delta}_i(t) = 0$ , for  $i = 1, \dots, n_e$ . Furthermore, it is

$$|\ddot{y}(t)| = \frac{\tau_{\max}}{J}, \quad (15)$$

and thus also all even derivatives of  $y$  from degree 4 to  $2n_e$ , amount to zero. Finally, since  $|\tau(t)| = \tau_{\max}$ , it is also  $y^{[2n_e+2]}(t) = 0$ . Consequently, during the phases at constant maximum torque, the trajectory  $y_d(t)$  for the flat output  $y$  will be a quadratic parabola with (absolute) curvature given by eq. (15).

With the above in mind, one can approach the problem by subdividing the interval of motion into five phases (A to E) as in Fig. 3, each defined by a polynomial trajectory for the output  $y$  satisfying suitable boundary conditions. The complete planned trajectory will be denoted as  $y_d(t)$  and the associated input torque as  $\tau_d(t)$ .

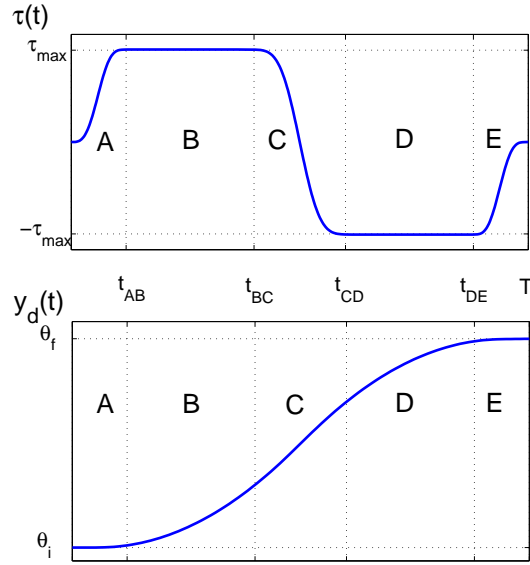


**Fig. 3** Subdivision of  $\tau(t)$  and  $y_d(t)$  in five planning phases

Given the input data, i.e., the required displacement  $\Delta\theta = \theta_f - \theta_i$ , the torque bound  $\tau_{\max}$ , and a desired  $T = T_{\min}$  (e.g., satisfying the relationship 13 of the rigid link case), one needs to define the five transition instants  $t_{AB}$ ,  $t_{BC}$ ,  $t_{CD}$  and  $t_{DE}$ . Due to motion symmetry, it will be  $t_{AB} = T - t_{DE}$  and  $t_{BC} = T - t_{CD}$ . Moreover, the problem will be reduced to the choice of the two normalized ratios

$$\tilde{T}_S := \frac{t_{AB}}{T}, \quad \tilde{T}_M := \frac{t_{CD} - t_{BC}}{T},$$

which will characterize the fraction of the total motion time devoted to the starting (or arriving) phase and, respectively, the fraction devoted to the midway phase. The choice of these fractions of the total time is left to the user (and this implies sub-optimality of the whole planning method).

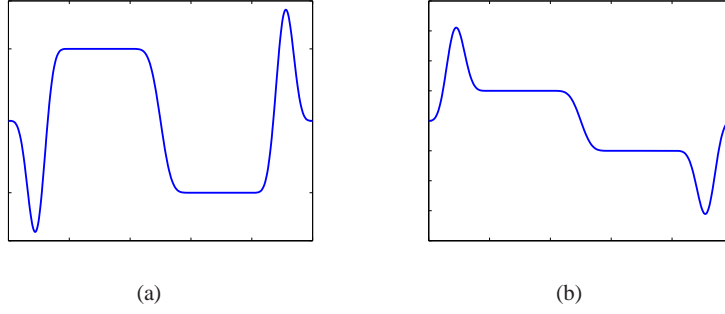


**Fig. 4** Under/overshooting of the torque due to overconstraining boundary conditions

However, this scheme will eventually encounter a problem of motion wandering and may fail to satisfy  $|\tau(t)| \leq \tau_{\max}$  during phases A and E, when the combination of input data is not properly set. This happens due to the fact that the linear system of equations defining the motion is overdetermined. If, e.g.,  $\tau_{\max}$  and  $T$  are chosen too large, the desired ‘smooth bang-bang’ torque profile would lead the arm too far and the solution has to counteract this by assembling torque peaks of opposite signs within phases A and E (see Fig. 4(a)). Similarly, if  $\tau_{\max}$  and  $T$  are chosen too small, these torque peaks will point in the other direction, exceeding  $\tau_{\max}$  in absolute value but assuring that the full torque profile will be sufficient to reach  $\theta_f$  (see Fig. 4(b)).

To overcome this problem, an efficient two-stage algorithm is devised which is based on: *i*) a first pass that computes a motion trajectory relaxing (normalizing) the constraint on maximum torque  $\tau_{\max}$  (case (a) below) or on motion time  $T$  (case (b) below), and evaluates the final angular displacement obtained (denoted as  $\Delta\theta^*$ ); *ii*) a suitable scaling of maximum torque (in case (a)) or, respectively, of motion time (in case (b)) based on  $\Delta\theta^*$ , and a second pass to recover the final desired motion.

### Solution algorithm

1. Input the values  $\Delta\theta = \theta_f - \theta_i$ , and the user’s choices  $\tilde{T}_S$  and  $\tilde{T}_M$ .
2. In case (a), input  $T$  and choose freely  $\tau_{\max}$ ; w.l.o.g., we define  $\tau_{\max} = 1$ ; in case (b), input  $\tau_{\max}$  and choose freely  $T$ ; w.l.o.g., we define  $T = 1$ .
3. Calculate the five polynomial segments of  $y_d(t)$  one after the other, matching the next phase to the end conditions of the previous one:

Phase A Polynomial of degree  $4n_e + 5$

$$\text{Left side: } y_d(0) = \dot{y}_d(0) = \ddot{y}_d(0) = \dots = y_d^{[2n_e+3]}(0) = 0$$

$$\text{Right side: } \ddot{y}_d(t_{AB-}) = \tau_{\max}/J, y_d^{[3]}(t_{AB-}) = \dots = y_d^{[2n_e+3]}(t_{AB-}) = 0$$

Phase B Quadratic parabola

$$\text{Left side: } y_d(t_{AB+}) = y_d(t_{AB-}), \dot{y}_d(t_{AB+}) = \dot{y}_d(t_{AB-})$$

With:  $\ddot{y}_d(t) = \tau_{\max}/J$ , for  $t \in [t_{AB}, t_{BC}]$

Phase C Polynomial of degree  $4n_e + 5$

Left side:  $y_d(t_{BC+}) = y_d(t_{BC-})$ ,  $\dot{y}_d(t_{BC+}) = \dot{y}_d(t_{BC-})$ ,  $\ddot{y}_d(t_{BC+}) = \tau_{\max}/J$ ,

$$y_d^{[3]}(t_{BC+}) = \dots = y_d^{[2n_e+3]}(t_{BC+}) = 0$$

Right side:  $\dot{y}_d(t_{CD-}) = -\tau_{\max}/J$ ,  $y_d^{[3]}(t_{CD-}) = \dots = y_d^{[2n_e+3]}(t_{CD-}) = 0$

Phase D Quadratic parabola

Left side:  $y_d(t_{CD+}) = y_d(t_{CD-})$ ,  $\dot{y}_d(t_{CD+}) = \dot{y}_d(t_{CD-})$

With:  $\ddot{y}_d(t) = -\tau_{\max}/J$ , for  $t \in [t_{CD}, t_{DE}]$

Phase E Polynomial of degree  $4n_e + 5$

Left side:  $y_d(t_{DE+}) = y_d(t_{DE-})$ ,  $\dot{y}_d(t_{DE+}) = \dot{y}_d(t_{DE-})$ ,  $\ddot{y}_d(t_{DE+}) = -\tau_{\max}/J$ ,

$$y_d^{[3]}(t_{DE+}) = \dots = y_d^{[2n_e+3]}(t_{DE+}) = 0$$

Right side:  $\ddot{y}_d(T) = \dots = y_d^{[2n_e+3]}(T) = 0$ .

4. Obtain a final angular displacement  $\Delta\theta^* = y_d(T)$ .

In case (a), set  $\tau_{\max} = \Delta\theta/\Delta\theta^*$  (instead of 1);

in case (b), set  $T = \sqrt{\Delta\theta/\Delta\theta^*}$  (instead of 1).

5. Repeat step 3 and exit with the resulting  $y_d(t)$  and derivatives.

The main clue of this algorithm is to predefine only the shape of  $y_d(t)$  and then scale it in a way that the displacement  $\Delta\theta$  is reached at the final time  $T$ . This works due to the linear relationship between the two state representations of the flexible arm system given in Sect. 3 and the homogeneity of the imposed boundary conditions. In case (a) the output trajectory computed in the first pass is stretched vertically, while in case (b) the computed torque is stretched horizontally.

As mentioned before, imposing zero boundary conditions up to  $y_d^{[2n_e+3]}$  will guarantee that the command torque obtained from eq. (12) will start and end at zero level and will have horizontal tangent at any transition instant (including initial and final time). Note also that there is no need to impose explicitly  $\dot{y}_d(T) = 0$ , as this will be automatically fulfilled by symmetry up to numerical rounding off. A final interesting observation is that the acceleration in each of the phases A, C, and E needs to satisfy only one non-zero boundary condition. As a consequence, by using doubly-normalized interpolating polynomials, one obtains only integer coefficients in the solution, providing thus numerical robustness. Moreover, the acceleration profile (and thus the torque) will never display overshooting effects for any time duration of these transition phases and for any number of flexible modes.

## 5 Numerical results

The solution algorithm has been applied to the same one-link flexible arm that was considered in [7] and has the following mechanical data:

$$\begin{aligned} \ell &= 0.7 \text{ m}, & \rho &= 2.975 \text{ kg/m}, & EI &= 2.4507 \text{ Nm}^2, \\ J_0 &= 1.95 \cdot 10^{-3} \text{ kgm}^2, & M_p &= 0.117 \text{ kg}, & J_p &= 0. \end{aligned}$$

For illustration, we considered the first  $n_e = 3$  modal frequencies of the flexible arm, which are  $f_1 = 4.05$ ,  $f_2 = 12.34$ , and  $f_3 = 22.87$  Hz, but numerically stable results have been obtained with up to eight modes.

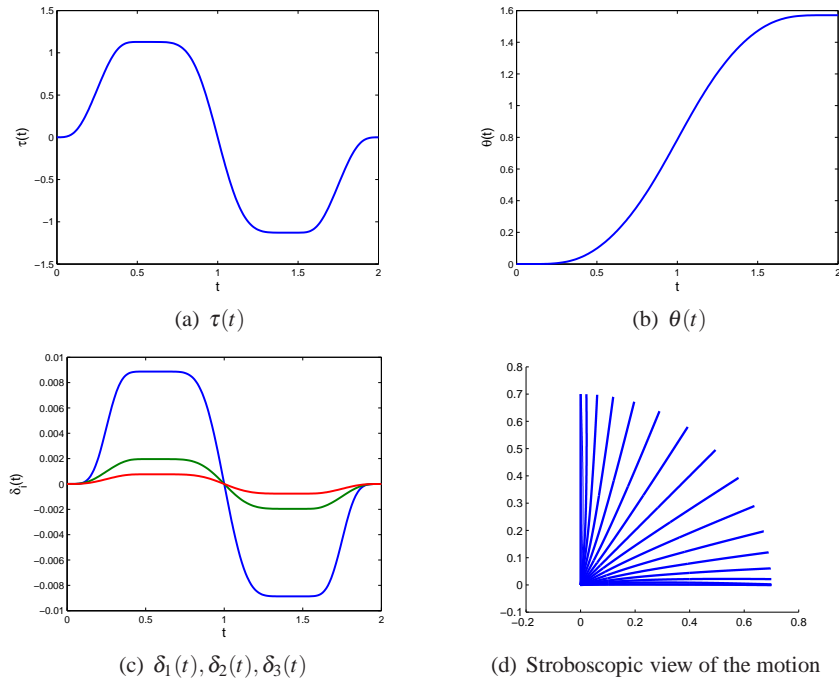


**Fig. 5** Numerical results for  $n_e = 3$  modes and assigned  $T = 2$  s of motion

Figure 5 shows the results for a rest-to-rest motion of  $\theta_f - \theta_i = \pi/2$  rad in  $T = 2$  s. The polynomials used in phases A, C, and E are of degree 17. The maximum absolute value of the torque obtained in the bang-bang phases B and D is  $\tau_{\max} = 1.2$  Nm, which is about 60% less than the single peak of torque obtained by pure polynomial interpolation in [7]. It is apparent that the flexible deformations definitely vanish at the desired final time. Indeed, if the problem was formulated as finding the minimum transfer time within this class of motions under the maximum

torque bound  $|\tau(t)| \leq 1.2$  Nm, the algorithm of Sec. 4 would have provided the same value of  $T = T_{\min} = 2$  s.

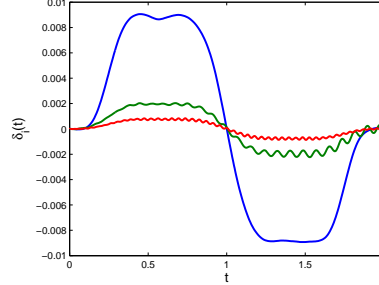


**Fig. 6** Evolution of the flexible variables when the nominal torque is disturbed by noise

In order to evaluate the effects of model perturbations, we have simulated the case when the nominally computed torque profile is superposed with noise whose amplitude amounts to 2% of the maximum torque. Figure 6 shows the associated evolution of the three flexible variables, which are close to zero but do not completely vanish at the final time  $T$ . To recover the final equilibrium configuration, it is enough to close a simple stabilizing PD feedback loop at the motor level

$$\tau = k_P(\theta_f - \theta_c) - k_D\dot{\theta}_c, \quad k_P, k_D > 0,$$

where  $\theta_c = \theta + \sum_{i=1}^{n_e} \phi_i'(0)\delta_i$  is the clamped angle at the flexible link base (see also Fig. 1), which can be measured by an encoder mounted on the motor [9]. Further numerical results can be found in [14], together with the Matlab/Simulink code.

## 6 Conclusions

We have presented a new method for calculating the nominal torque required for rest-to-rest motion of a one-link flexible arm in a given time, and approximately minimizing the maximum torque, or under a given torque constraint, and approximately minimizing the motion time. The method is based on the existence of a flat output  $y$  for the system such that the evolution of all original state variables (rigid and flexible motion) of the arm is uniquely associated to this output and to a finite number of its time derivatives. By analogy with the rigid case, the solution uses at best the actuator capacity by smoothing a bang-bang torque profile around the initial, midpoint, and final instants with polynomials of appropriate order and boundary conditions. A two-stage algorithm has been implemented exploiting time or torque scaling, so as to prevent the undesired formation of motion wandering during the smoothing phases.

The approach is fully developed in the time domain and lends itself to several generalizations, including the smoothing of bang-coast-bang torque profiles under an additional constraint of maximum velocity, the combination with a stabilizing feedback law for compensating disturbances and small modeling errors, the consideration of modal damping, and the extension to nonlinear multi-body flexible dynamics.

**Acknowledgements** This work was performed while the second author was visiting the Department of Computer and Systems Sciences (DIS) of the Università di Roma “La Sapienza” under the *ERASMUS* program.

## References

1. Bhat, S. P., Miu, D. K.: Precise point-to-point positioning control of flexible structures. *ASME J. of Dynamic Systems, Measurements, and Control*, **112**, 667–674 (1990)
2. Bellezza, F., Lanari, L., Ulivi, G.: Exact modeling of the flexible slewing link. in *Proc. 1990 IEEE Int. Conf. on Robotics and Automation*, pp. 734–739 (1990)
3. Book, W. J.: Modeling, design, and control of flexible manipulator arms: A tutorial review, in *Proc. 29th IEEE Conf. on Decision and Control*, pp. 500–506 (1990)
4. Bremer, H.: *Dynamik und Regelung mechanischer Systeme*. Teubner, Stuttgart (1988)
5. De Luca, A., Siciliano, B.: Flexible Links. In: Canudas de Wit, C., Siciliano, B., Bastin G. (eds.) *Theory of Robot Control*, pp. 219–261. Springer Verlag, Berlin (1996)
6. De Luca, A.: Feedforward/feedback laws for the control of flexible robots. in *Proc. 2000 IEEE Int. Conf. on Robotics and Automation*, pp. 233–240 (2000)
7. De Luca, A., Di Giovanni, G.: Rest-to-rest motion of a one-link flexible forearm. *Proc. 2001 IEEE/ASME Int. Conf. on Advanced Mechatronics*, pp. 923–928 (2001)
8. De Luca, A., Di Giovanni, G.: Rest-to-rest motion of a two-link robot with a flexible forearm. *Proc. 2001 IEEE/ASME Int. Conf. on Advanced Mechatronics*, pp. 929–935 (2001)
9. De Luca, A., Caiano, V., Del Vecovo, D.: Experiments on rest-to-rest motion of a flexible arm. In: Siciliano, B., Dario P. (eds.) *Experimental Robotics VIII*, Springer Tracts in Advanced Robotics, vol. 5, pp. 338–349. Springer Verlag, Berlin (2003)
10. De Luca, A., Oriolo, G., Vendittelli, M., Iannitti, S.: Planning motions for robotic systems subject to differential constraints. In: Siciliano, B., De Luca, A., Melchiorri, C., Casalino, G. (eds.) *Advances in Control of Articulated and Mobile Robots*, Springer Tracts in Advanced Robotics, vol. 10, pp. 1–38. Springer Verlag, Berlin (2004)
11. Gebler, B.: Modellbildung, Steuerung und Regelung für elastische Industrieroboter. *VDI Fortschrittsbericht Reihe 11*, nr. 98 (1987)
12. Kwon, D.-S., Book, W. J.: An inverse dynamic method yielding flexible manipulator state trajectories. in *Proc. 1990 American Control Conf.*, pp. 186–193 (1990)
13. Norton, R. L.: *Cam Design and Manufacturing Handbook*, Industrial Press, New York (2002)
14. Panzer, H.: Rest-to-rest motion of a one-link flexible arm with smooth bang-bang torque profile. *TUM – Lehrstuhl für Angewandte Mechanik Semesterarbeit*, Technische Universität München (2008)
15. Singer, N. C., Seering, W. P.: Preshaping command inputs to reduce system vibration. *ASME J. of Dynamic Systems, Measurements, and Control*, **112**, 76–82, (1990)
16. Yang, H., Krishnan, H., Ang Jr., M. H.: A simple rest-to-rest control command for a flexible link robot. in *Proc. 1997 IEEE Int. Conf. on Robotics and Automation*, pp. 3312–3317 (1997)